

# Exploring Part-Informed Visual-Language Learning for Person Re-Identification

Yin Lin<sup>1,2</sup>, Cong Liu<sup>2</sup>, Yehansen Chen<sup>2</sup>, Jinshui Hu<sup>2</sup>, Bing Yin<sup>2</sup>, Baocai Yin<sup>2</sup>, Zengfu Wang<sup>1\*</sup>

<sup>1</sup> Department of Automation, University of Science and Technology of China, Hefei, China

<sup>2</sup> iFLYTEK Research, Hefei, China

lin5875@mail.ustc.edu; zfwang@ustc.edu.cn;

{yinlin, congliu2, yhschen, jshu, bingyin, bcyin}@iflytek.com

## Abstract

Recently, visual-language learning has shown great potential in enhancing visual-based person re-identification (ReID). Existing visual-language learning-based ReID methods often focus on whole-body scale image-text feature alignment, while neglecting supervisions on fine-grained part features. This choice simplifies the learning process but cannot guarantee within-part feature semantic consistency thus hindering the final performance. Therefore, we propose to enhance fine-grained visual features with part-informed language supervision for ReID tasks. The proposed method, named **Part-Informed Visual-language Learning** ( $\pi$ -VL), suggests that (i) a human parsing-guided prompt tuning strategy and (ii) a hierarchical fusion-based visual-language alignment paradigm play essential roles in ensuring within-part feature semantic consistency. Specifically, we combine both identity labels and parsing maps to constitute pixel-level text prompts and fuse multi-stage visual features with a light-weight auxiliary head to perform fine-grained image-text alignment. As a plug-and-play and inference-free solution, our  $\pi$ -VL achieves substantial improvements over previous state-of-the-arts on four common-used ReID benchmarks, especially reporting **90.3% Rank-1** and **76.5% mAP** for the most challenging MSMT17 database without bells and whistles.

## 1. Introduction

Person re-identification (ReID) refers to the task of retrieving the query person-of-interest from large-scale gallery databases captured by non-overlapping camera views [56]. Owing to its practical importance for intelligent video surveillance, ReID has gained ever-growing attention from both academia and industry in recent years [34, 44, 49].

Appearance feature learning [15, 37, 66] is a good starting point for ReID, as appearance biometrics serve as the

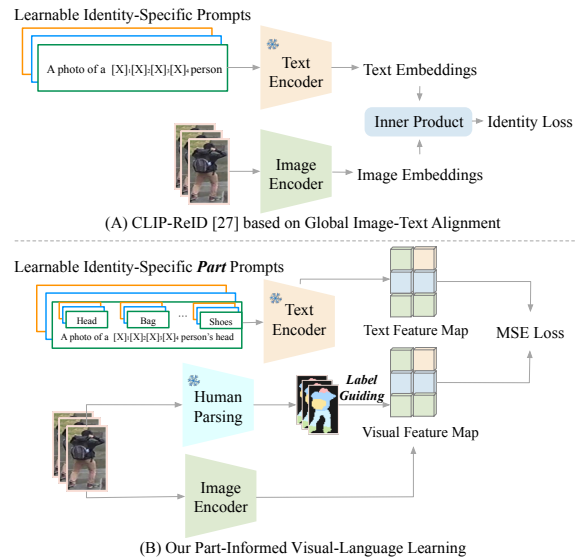


Figure 1. Comparison of CLIP-ReID [27] and our part-informed vision-language learning framework. (a) CLIP-ReID based on Global Image-Text Alignment. (b) Our Part-Informed Visual-Language Learning.

most fundamental and well-studied cues for identity recognition tasks [34]. In addition, the accumulation of high-quality image databases and manual annotations [49, 60, 61] endows neural networks the robustness to different illuminations, poses, viewpoints and backgrounds. Nowadays, appearance-based ReID has achieved considerable success on a wide range of applications [56]. Nevertheless, appearance feature learning should not be the end point for ReID. Since human body semantics are not apparently reflected by the raw pixel distribution [4], it is hard to directly learn semantic information under the single supervision from fixed sets of one-hot identity labels [27].

Inspired by the recent success of vision-language models [24, 38], CLIP-ReID [27] is one of the pioneer attempts that leverages natural texts to specify visual concepts beyond appearance. By tuning identity-specific text prompts [65], it

\*Corresponding author

uses text representations generated by a powerful text encoder [38] to deliver the image encoder a broader source of supervision, leading to more discriminative global features. However, naively porting ideas from global image-text alignment may not suffice for ReID. Several studies [29, 44, 53] have demonstrated that some non-salient details can be easily overwhelmed, raising *within-part semantic inconsistency* (see Fig. 2), while mining part-informed visual features is a promising solution [44]. Meanwhile, natural language inherently possesses a higher information density to depict fine-grained characteristics of body parts [70]. This motivates us to think: *Is learning part-informed semantics as easy as global image-text alignment?*

An obstacle to answering this question lies in the ambiguous boundaries between different human body parts, which hampers the identification of visual features with the same part semantics. This problem, however, has largely been solved by state-of-the-art human parsing models [26, 55]. With human parsing, each pixel in a person image can be easily transformed to a specific semantic category, *e.g.*, head, face, shoes. This enables us to generate high-quality text prompts based on local parsing semantics and perform fine-grained text-image alignment.

When ReID models are able to learn fine-grained semantics with parsing-enabled natural language supervision, however, a *supervision conflict* problem arises. That is, human parsing only distinguishes *identity-agnostic* body part semantics, while ReID requires us to learn *identity-specific* discriminative cues [52]. Such conflict will pull features of the same body parts into corresponding clusters, whereas suppressing the feature diversity and confusing the decision boundary of identity recognition.

In this paper, we address the above problems by introducing a **Part-Informed Vision-Language** learning framework, named  $\pi$ -VL, for general person ReID tasks. Unlike existing works that apply parsing maps for background clutter elimination [43] or body alignment [9], we propose to construct part-informed text prompts via human parsing, and perform per-pixel image-text alignment to enhance RGB-based ReID. To alleviate the *supervision conflict* problem, we combine both identity and parsing text tokens for prompt tuning, leading to more discriminative part descriptions. Furthermore, considering the hierarchical feature extraction nature of visual backbones, we propose a light-weight auxiliary head to fuse multi-stage visual features for semantic enhancement. It is worth noting that  $\pi$ -VL is a plug-and-play and loss function-based solution, it is highly compatible with existing RGB-based ReID models.

Experimental results on both CNN and ViT-based backbones suggest that  $\pi$ -VL has the potential to be used as a universal front-end capable of handling various application scenarios. It sets new state-of-the-art *i.e.*, **90.3%** Rank-1 and **76.5%** mAP, on the MSMT17 benchmark, and shows

consistent improvements over mainstream ReID databases.

Our main contributions are summarized as follows:

- We propose a part-informed vision-language learning framework, named  $\pi$ -VL, for RGB-based person ReID. To the best of our knowledge, this is one of the first attempts to introduce fine-grained visual-language learning for ReID tasks.
- We present an identity-aware part-informed prompt tuning strategy via human parsing. With this strategy, we can generate pixel-level text prompts based on both identity labels and parsing maps, strengthening the visual encoder to spot more discriminative features.
- We design a hierarchical fusion-based alignment mechanism to conduct image-text alignment in a parallel multi-stage manner, resulting in a more semantic meaningful feature space for person image retrieval.
- Extensive experiments on mainstream RGB-based ReID benchmarks not only demonstrate the superior performance of the proposed method, but also validate its generalization ability to various visual backbones.

## 2. Related Work

### 2.1. Appearance-based Person ReID

Appearance-Based ReID aims to match a target pedestrian across disjoint visible camera views at varying places and times. It is challenging to learn suitable feature representations robust enough to withstand large intra-class variations of illumination [57], poses [35], scales [17], viewpoints [21] and background clutter [33]. Earlier studies often utilize handcrafted descriptors (*e.g.*, HOG [6] and LOMO [31]) to extract low-level features such as color, shape, or texture for person retrieval. However, it is pretty hard to manually design optimal visual features with stronger discriminability and better stability [54].

Nowadays, deep learning methods show powerful capacity of automatically extracting features from large-scale image datasets and have achieved state-of-the-art results on RGB-based person ReID tasks [17, 35, 54]. Building on various sophisticated CNN architectures, deep ReID models are doing exceptionally well on visual matching by learning robust cross-camera feature representations and optimal distance metrics in an end-to-end manner [3, 5, 34, 56].

To learn more discriminative features, part information and contextual information are also exploited in recent works [20, 33, 35, 42, 48]. For example, methods like PCB [44] and MGN [53] utilize hand-crafted partitioning to split feature maps into grid cells or horizontal stripes for local feature learning. Another line of researches adopt off-the-shelf pose estimation [48] or attention module [28] to extract the human part aligned features. Although these

approaches have reported encouraging performance, the learned part features still lack high-level semantics under the single supervision of discrete identity labels [27].

## 2.2. Visual-language Pretraining

Over the past years, the emergence of vision-language pre-training models [18, 24, 25, 38] has led to substantial improvements to many downstream tasks [13, 14]. Based on the idea of contrastive image-text alignment, CLIP [38] exploits a two-directional InfoNCE loss [36] to pretrain a pair of image and text encoders, leading to semantic meaningful visual representations in harmony with manually-designed text prompts. Motivated by the success of CLIP, several works propose to incorporate different types of pretraining objectives, such as image-to-text matching [24] and mask image-text modeling [22], to learn more universal visual-language representations.

To fully excite the potential of vision-language pretraining models with negligible computation costs, prompt or adapter-based tuning has also been investigated by many researchers. For example, CoOp [65] suggests that learning dataset-specific text prompts contributes to better image classification accuracy than manual prompt engineering. CoCoOp [64] extends CoOp by learning a lightweight meta-network to generate an input-conditional token for each image. CLIP-adapter [10] inserts a plug-and-play bottleneck layer and performs residual feature blending on top of pretrained image and text encoders.

Thanks to the above efforts, nowadays, CLIP-pretrained models have been widely applied to a wide range of downstream tasks, *e.g.*, object detection [12], semantic segmentation [39], and image retrieval [1]. To our best knowledge, CLIP-ReID [27] is the first milestone that deals with ReID tasks based on CLIP. By tuning identity-specific text prompts [65], it uses text representations generated by a powerful text encoder [38] to distill the image encoder, leading to more discriminative global features. However, the local part features still lack meaningful semantics under the only supervision of global identity text embeddings.

## 3. Methodology

In this section, we first depict an overview of the baseline model, *i.e.*, CLIP-ReID (Section 3.1) and illustrate the within-part semantic inconsistency problem (Section 3.2). Then, we elaborate on our main contributions: (a) an identity-aware part-informed prompt tuning strategy that generates pixel-level text prompts for fine-grained visual-language learning (Section 3.3), and (b) hierarchical fusion-based alignment (Section 3.4) for visual-language learning.

### 3.1. Preliminaries: Overview of CLIP-ReID

CLIP-ReID [27] is the first milestone that applies vision-language pretraining models to image-based ReID. As one-

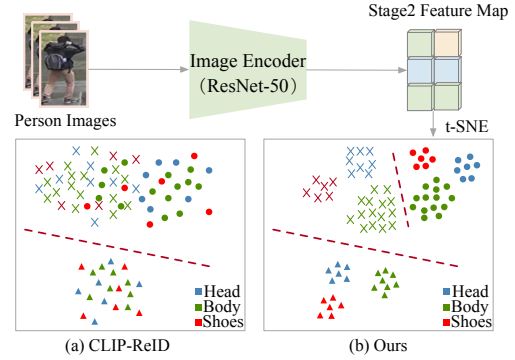


Figure 2. Illustration of within-part semantic inconsistency. Colors indicate different body parts, symbols denote human identities, and the red dashed line represents the decision boundary for identity recognition. It can be observed that features of different body parts are hard to distinguish via global image-text alignment (Fig.2(a)), while fine-grained visual-language learning serves as a promising solution (Fig.2(b)).

hot identity labels used by ReID are meaningless to construct high-quality text prompts, CLIP-ReID proposes a two-stage training procedure to invest global visual features with natural language supervision.

The first training stage aims to optimize identity-specific text tokens with CLIP-style supervision. By passing a pre-designed text description  $T_D = \text{'A photo of a } [X]_1 [X]_2 [X]_3 \dots [X]_M \text{ person.}'$  and the corresponding person image  $I_i$  through a *frozen* text encoder  $\mathcal{T}(\cdot)$  and a *frozen* image encoder  $\mathcal{I}(\cdot)$  respectively, a text embedding  $T_{y_i}$  and an image embedding  $V_{y_i}$  could be obtained by:

$$T_{y_i} = \mathcal{T}(T_D); \quad V_{y_i} = \mathcal{I}(I_i), \quad (1)$$

where  $[X]$  denotes a learnable text token with the word embedding dimension,  $M$  is the number of learnable text tokens, and  $y_i$  indicates the identity label.

Then CLIP-style contrastive learning losses  $\mathcal{L}_{i2t}$  and  $\mathcal{L}_{t2i}$  [38] are computed to optimize  $[X]_1 [X]_2 [X]_3 \dots [X]_M$ :

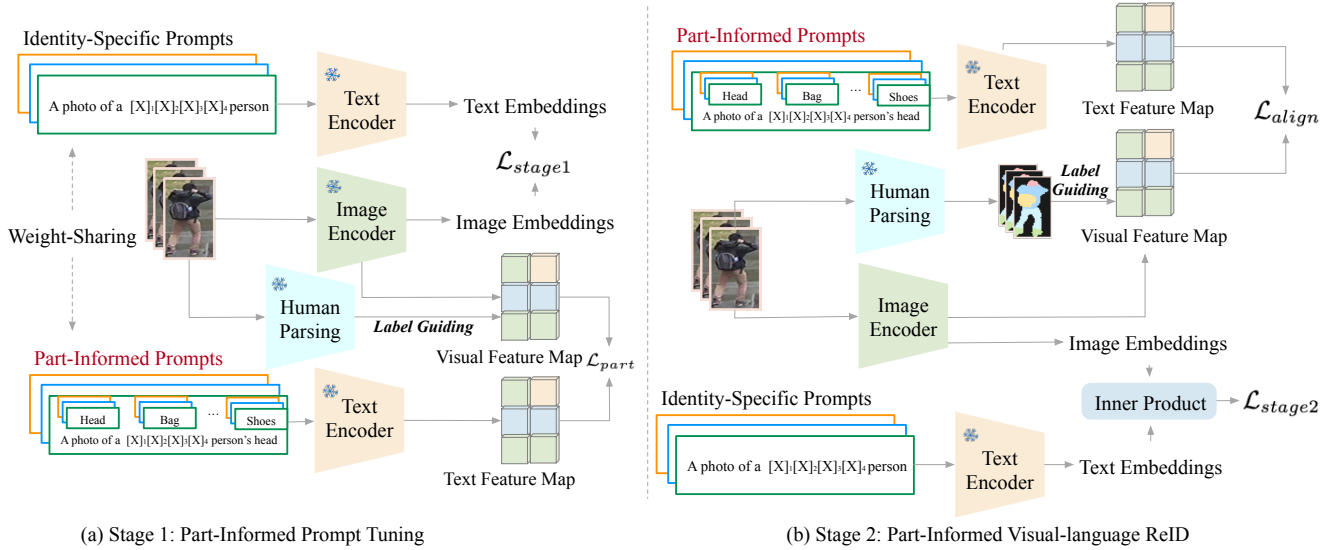
$$\mathcal{L}_{stage1} = \mathcal{L}_{i2t} + \mathcal{L}_{t2i}. \quad (2)$$

In the second training stage, the learned identity-specific text embeddings are treated as a *classifier*, and the image encoder  $\mathcal{I}(\cdot)$  is fully optimized under the supervision of identity loss  $\mathcal{L}_{id}$  with label smoothing and triplet loss  $\mathcal{L}_{tri}$  [34]:

$$\mathcal{L}_{i2tce} = \sum_{k=1}^N -q_k \log \frac{\exp(V_i \cdot T_{y_k})}{\sum_{y_a=1}^N \exp(V_i \cdot T_{y_a})} \quad (3)$$

$$\mathcal{L}_{stage2} = \mathcal{L}_{id} + \mathcal{L}_{tri} + \mathcal{L}_{i2tce}, \quad (4)$$

where  $q_k$  represents the soft label in the target distribution,  $N$  is the number of identities, and  $i$  denotes the image index.



(a) Stage 1: Part-Informed Prompt Tuning

(b) Stage 2: Part-Informed Visual-language ReID

Figure 3. The proposed  $\pi$ -VL framework. To solve the within-part semantic inconsistency issue (Section 3.2), it first learns identity-specific and part-informed text prompts in a coarse-to-fine manner (Section 3.3). Then it leverages a hierarchical fusion-based alignment strategy (Section 3.4) to perform fine-grained image-text alignment between part-informed text embeddings and multi-scale visual features.

### 3.2. Within-part Semantic Inconsistency

CLIP-ReID is simple and effective, yet to be improved. Since the natural language supervision is limited to the whole-body scale (Eq.(3)), some non-salient or infrequent part features can be easily overwhelmed, and still lack high-level semantics [49]. As shown in Fig.2, we use t-SNE [46] to visualize the pixel-level feature distributions of CLIP-ReID models on DukeMTMC [40], and adopt human parsing [26] to assign semantic labels for each pixel (see the appendix for details). Colors indicate different body parts, while symbols denote human identities.

We observe that although the decision boundary of identities (the red dashed line) is generally clear, features of different body parts are hard to distinguish. Furthermore, for several confusing identities (e.g., identities denoted as crosses and circles), the classification boundary of their part features is even more difficult to be recognized. We term this issue as *within-part semantic inconsistency*, which directly hinders the performance of person retrieval.

### 3.3. Part-informed Prompt Tuning

An intuition to solve the within-part semantic inconsistency issue is to pull together part features with the same semantic, while pushing apart irrelevant counterparts. This intuition, however, further raises two questions: (1) How to identify the semantics of fine-grained part features? (2) How to design the supervision signal for part distinction?

The first question has already been answered by state-of-the-art human parsing models robust to the ambiguous boundaries between different body parts. Thus, we employ

a human parsing model  $\mathcal{H}$  [26] to generate pixel-level parsing maps  $P$  for person image  $I_i$ :

$$P = \mathcal{H}(I_i), \quad P \in \mathbb{R}^{H \times W}, \quad (5)$$

where  $H / W$  denotes the height / width of  $I_i$ , respectively. By doing this, we classify each pixel of the input image into 20 semantic categories, including ‘Background’, ‘Hat’, ‘Hair’, etc (see the appendix for details). This allows us to generate per-pixel text prompts based on these semantic labels and the pretrained text encoder of CLIP.

However, human parsing inherently sets a new obstacle to answering the second question. That is, human parsing only distinguishes *identity-agnostic* body part semantics, while ReID requires us to learn *identity-specific* discriminative cues [52]. This conflict will suppress the diversity and discriminability of ReID features to some extent, leading to inferior performance.

Inspired by [65], we propose a part-informed prompt tuning strategy to solve the supervision conflict issue. As illustrated in Fig.3(a), like [27], we first learn identity-specific tokens with the text prompt  $T_i$ , i.e., ‘A photo of a  $[X]_1[X]_2[X]_3 \dots [X]_M$  person’, through optimizing Eq.(2). But unlike [27], after warm-up tuning with Eq.(2), we reformulate the learned prompts with parsing maps to generate pixel-level part prompts. Suppose we have the parsing map  $P \in \mathbb{R}^{H \times W}$  and the identity prompt  $T_i$  of a person image  $I_i$ , we can obtain the part text-embedding  $T_i^{part}$  by:

$$\begin{aligned} T_i^{part} &= \mathcal{T}(\text{concat}(T_i, L(p))), \quad p \in P, \\ T_i^{full} &= \text{aggregate}(T_i^{part}) \quad T_i^{full} \in \mathbb{R}^{H \times W}, \end{aligned} \quad (6)$$

where  $L(\cdot)$  indicates the tokenize operator for parsing label text (e.g., ‘head’),  $\text{concat}(\cdot, \cdot)$  represents the concatenation of text tokens, and  $\text{aggregate}(\cdot)$  means the pixel-level concatenation of text embeddings.

Inspired by [51], we propose to learn our part-informed text prompts with pixel-level dense contrastive learning. Specifically, we treat text and visual embeddings of the same person and the same body part  $(t_i, v_{i+})$ ,  $(v_i, t_{i+})$  as positive pairs, while counting the others as negative pairs  $(t_i, v_{i-})$ ,  $(v_i, t_{i-})$ :

$$\mathcal{L}_{t2i}^{part} = \frac{1}{H \times W} \sum_{i=1}^{H \times W} \log \frac{\exp(t_i \cdot v_{i+} / \tau)}{\exp(t_i \cdot v_{i+}) + \sum_{v_{i-}} \exp(t_i \cdot v_{i-} / \tau)},$$

$$\mathcal{L}_{i2t}^{part} = \frac{1}{H \times W} \sum_{i=1}^{H \times W} \log \frac{\exp(v_i \cdot t_{i+} / \tau)}{\exp(v_i \cdot t_{i+}) + \sum_{t_{i-}} \exp(v_i \cdot t_{i-} / \tau)},$$

$$\mathcal{L}_{part} = \mathcal{L}_{t2i}^{part} + \mathcal{L}_{i2t}^{part}, \quad (7)$$

$$\mathcal{L}_{prompt} = \mathcal{L}_{stage1} + \mathcal{L}_{part}, \quad (8)$$

where  $\tau$  is the temperature coefficient of the InfoNCE loss. During the prompt tuning process, only the learnable text tokens  $[X]_1[X]_2[X]_3 \dots [X]_M$  are optimized, while the image and text encoders are frozen.

### 3.4. Hierarchical Fusion-based Alignment

With part-informed prompt tuning, we are able to yield identity-specific text embeddings with body semantics. However, when performing image-text alignment, there is still an open issue on the acquisition manner of visual features. Previous works suggest that image encoders inherently form a hierarchical feature space with both low-level and high-level semantics [14]. Therefore, we propose to fuse multi-scale pyramidal visual features for dense image-text alignment. Considering the real-time application of ReID networks, we design a hierarchical fusion-based alignment module that brings *no additional computation costs* for model inference.

Fig.4 illustrates the basic idea of our hierarchical fusion-based alignment strategy. For CNN-based backbones, e.g., ResNet-50 [14], we denote the output of last residual blocks for conv2, conv3, conv4 outputs as  $\{C2, C3, C4\}$ . Considering the parameter efficiency, we simply attach a  $1 \times 1$  depth-wise convolution *i.e.*,  $DW(\cdot)$  [41], to align the channel dimension of the output features (Fig.4(a)), denoted as:

$$F_i = DW(C_i), \quad i \in \{2, 3, 4\}. \quad (9)$$

Then we use downsampling or upsampling operations to align the spatial dimensions of output features to stride=8:

$$F_2 = \text{downsample}(F_2), F_4 = \text{upsample}(F_4), \quad (10)$$

$$F_{out} = F_2 + F_4.$$

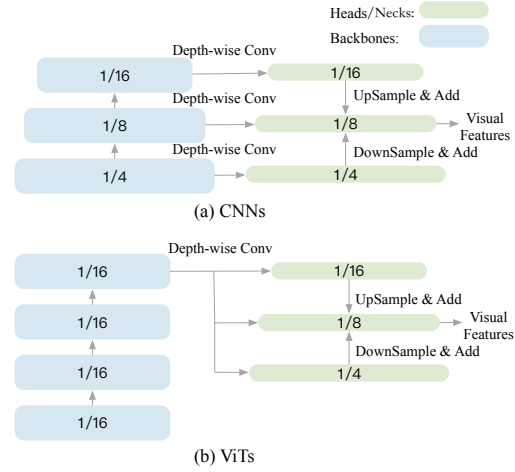


Figure 4. Illustration of the hierarchical fusion-based alignment strategy. Inspired by [32] and [30], we propose to fuse multi-scale features of CNNs and ViTs for image-text alignment.

For ViT-based backbones [8], we follow the design principle proposed by [30] (see Fig.4(b) for details) to fuse multi-scale visual features for a plain backbone.

Here, we obtain pixel-level image and text feature pairs  $(F_{out}, T^{full})$ , and the image-text alignment is implemented with a simple mean squared error loss, *i.e.*,

$$\mathcal{L}_{align} = \|F_{out} - T^{full}\|_2^2. \quad (11)$$

The overall learning objective of the second training stage is a weighted summation of ReID loss (Eq.(4)) and pixel-level image-text alignment loss  $\mathcal{L}_{align}$ , defined as:

$$\mathcal{L}_{overall} = \mathcal{L}_{id} + \mathcal{L}_{tri} + \mathcal{L}_{i2tce} + \mathcal{L}_{align}. \quad (12)$$

## 4. Experiments

In this section, we first introduce our experimental databases, evaluation protocols, and implementation details. Then, the proposed framework is compared with several state-of-the-art methods. Finally, we conduct ablation studies to investigate the contribution of each component and analyze some visualization results.

### 4.1. Datasets and Evaluation Protocols

Table 1. Statistics of the experimental databases.

Dataset	#ID	#Person Image	#Camera
MSMT17 [53]	4,101	126,441	15
Market-1501 [60]	1,501	32,668	6
DukeMTMC [40]	1,404	36,411	8
Occluded-Duke [35]	1,404	35,489	8

We evaluate the proposed method on four publicly available person ReID benchmarks, including MSMT17 [53],

Market-1501 [60], DukeMTMC [40], and Occluded-Duke [35]. Table 1 presents an overview of the included datasets. We follow the general evaluation protocol [60] for RGB-based person ReID. The standard cumulated matching characteristics (CMC) curve and mean average precision (mAP) are used to evaluate the retrieval performance.

## 4.2. Implementation Details

We implement the proposed method with PyTorch and conduct training on one NVIDIA V100-32G GPU. For fair comparisons, we generally follow the experimental setting of [27] and keep all default hyper-parameters unchanged. Specifically, the pretrained image and text feature extractors of CLIP [38] are adopted as the backbone of our visual and text encoders respectively. For the visual encoder, we choose ResNet-50 with the last stride=1 and global attention pooling, and ViT-B/16 with 12 transformer blocks to meet the common practice of existing CNN-based and ViT-based ReID works [15, 34]. For the text encoder, we directly adopt the version provided by [38]. The dimensions of the image and text embeddings are aligned to 1024 with a linear layer to conduct vision-language learning.

In the first training stage, we only optimize the learnable text prompts using Adam during a total of 80 epochs (60 for identity-aware prompt tuning and 20 for part-informed prompt tuning), while keeping the other network parameters fixed. The learning rate is initialized at  $3.5 \times 10^{-4}$  and tuned by a cosine decay schedule. We randomly sample 16 identities with 4 images per person, resulting in 64 images for each training batch. All the input images are resized to  $256 \times 128$  (*i.e.*, height  $\times$  width) without data augmentation.

For the second training stage, the batch sampling strategy is kept unchanged, whereas each image is padded with 10 pixels and augmented with random cropping, horizontal flipping, and erasing [62] to  $256 \times 128$ . The CNN-based model is trained for 120 epochs while the ViT-based model is trained for 60 epochs. For the CNN version, we adopt a warm-up strategy [34], and the initial learning rate is set to  $3.5 \times 10^{-4}$  and decays by 0.1 and 0.01 at the 40th and 70th epoch. For the ViT version, the same warm-up strategy is utilized, the initial learning rate is set to  $5 \times 10^{-6}$  and decays by 0.1 and 0.01 at the 30th and 50th epoch. The margin of triplet loss in Eq.(4) is set as 0.3.

## 4.3. Comparisons with State-of-the-arts

In this subsection, we demonstrate the effectiveness of our proposed method by comparing it with state-of-the-arts. The compared approaches include global visual representation learning methods [11, 23, 27, 37, 45, 50, 58, 59, 66], local visual representation learning models [2, 19, 29, 44, 48, 49, 68], and ViT-based approaches [15, 27, 67, 69]. Since most of them follow the same evaluation protocols, we directly report their results from the published papers.

Table 2 demonstrates the Rank-1 accuracy and mAP of different methods on the 4 included datasets. Generally, we have the following observations:

### ‘Local’ performs generally better than ‘Global’.

Compared with global visual representation learning methods, the local feature learning counterparts generally present better ReID performance. For example, on MSMT17, ABD-Net gets 3.4% absolute Rank-1 improvements over CDNet. This suggests that introducing part-informed network structures or supervisions do enhance the discriminability of the learned features. Moreover, finer feature learning granularity forms a more discriminative feature space (*e.g.*, MGN *vs* PCB). All these motivate us to design fine-grained visual-language supervisions for ReID.

### ViT severs as a more powerful backbone than CNN.

As shown in the bottom rows of Table 2, ViT-based models outperforms CNN-based ones by a large margin. This is highly predictable owing to the long-term perceptual capacity of the self-attention mechanism [47]. In addition, the ‘position embedding’ paradigm further enables us to encode useful auxiliary information like camera views [15] to the learned representations. It is worth noting that, our proposed method is compatible with both CNN and ViT-based network structures, leading to higher generalization ability.

### Visual-language learning benefits RGB-based ReID.

As proven by CLIP-ReID, a pair of feature-aligned image and text encoders bring substantial enhancement to ReID tasks. Specifically, on MSMT17, it demonstrates 4.4% absolute improvements against TransReID. On the one hand, the broader supervision provided by natural language effectively enhances the semantics of visual features. Moreover, CLIP provides a better starting point than traditional ImageNet supervised pretraining [14] used by ReID models. However, CLIP-ReID only imparts natural language supervision on the global visual features, which overlooks the fine-grained semantics of fine-grained part features.

### Part-Informed visual-language learning matters.

Our  $\pi$ -VL surpasses all the prior CNN and ViT-based state-of-the-arts on all four experimental benchmarks. All the results are achieved under the single-query mode without re-ranking or other bells and whistles. Notably, we achieve **90.3%** Rank-1 and **76.5%** mAP for MSMT17, setting new state-of-the-art on this database. This indicates that introducing part-informed text prompts does lead to more semantic meaningful visual features. Furthermore, all the improvements are achieved without FLOPs or parameters increase, which exhibits the generalization ability of  $\pi$ -VL.

## 4.4. Ablation Studies

In this section, we evaluate the effectiveness of different  $\pi$ -VL components. The ablation results on DukeMTMC are summarized in Table 3. Here we adopt CLIP-ReID as the baseline model. To evaluate the effect of part-informed

Table 2. Comparison with state-of-the-art CNN- and ViT-based methods on person ReID datasets.

Backbone	Methods	Venues	MSMT17		Market-1501		DukeMTMC		Occluded-Duke	
			mAP	Rank-1	mAP	Rank-1	mAP	Rank-1	mAP	Rank-1
CNN	PCB [44]	ECCV 2018	-	-	81.6	93.8	69.2	83.3	-	-
	MGN [49]	MM 2018	-	-	86.9	95.7	78.4	88.7	-	-
	OSNeT [66]	ICCV 2019	52.9	78.7	84.9	94.8	73.5	88.6	-	-
	ABD-Net [2]	ICCV 2019	60.8	82.3	88.3	95.6	78.6	89.0	-	-
	Auto-ReID [37]	ICCV 2019	52.5	78.2	85.1	94.5	-	-	-	-
	HOReID [48]	CVPR 2020	-	-	84.9	94.2	75.6	86.9	43.8	55.1
	ISP [68]	AAAI 2020	-	-	88.6	95.3	80.0	89.6	52.3	62.8
	SAN [19]	AAAI 2020	55.7	79.2	88.0	96.1	75.5	87.9	-	-
	OfM [58]	AAAI 2021	54.7	78.4	87.9	94.9	78.6	89.0	-	-
	CDNet [23]	CVPR 2021	54.7	78.9	86.0	95.1	76.8	88.6	-	-
	PAT [29]	CVPR 2021	-	-	88.0	95.4	78.2	88.8	53.6	64.5
	CAL [11]	ICCV 2021	56.2	79.5	87.0	94.5	76.4	87.2	-	-
	CBDB-Net [45]	TCSVT 2021	-	-	85.0	94.4	74.3	87.7	38.9	50.9
	ALDER [59]	TIP 2021	59.1	82.5	88.9	95.6	78.9	89.9	-	-
	LTReID [50]	TMM 2022	58.6	81.0	89.0	95.9	80.4	90.5	-	-
CLIP-ReID [27]	AAAI 2023	63.0	84.4	89.8	95.7	80.7	90.0	53.5	61.0	
$\pi$ -VL (Ours)	-	<b>63.8</b>	<b>85.0</b>	<b>90.2</b>	<b>96.1</b>	<b>81.3</b>	<b>91.2</b>	<b>54.0</b>	<b>61.8</b>	
ViT	AAformer [69]	Arxiv 2021	63.2	83.6	87.7	95.4	80.0	90.1	58.2	67.0
	TransReID [15]	ICCV 2021	67.4	85.3	88.9	95.2	82.0	90.7	59.2	66.4
	DCAL [67]	CVPR 2022	64.0	83.1	87.5	94.7	80.1	89.0	-	-
	CLIP-ReID [27]	AAAI 2023	75.8	89.7	90.5	95.4	83.1	90.8	60.3	67.2
	$\pi$ -VL (Ours)	-	<b>76.5</b>	<b>90.3</b>	<b>91.2</b>	<b>96.2</b>	<b>84.0</b>	<b>92.1</b>	<b>61.0</b>	<b>68.3</b>

visual-language learning, we first only employ the semantic labels generated by human parsing as the text prompt  $\mathcal{H}$ , resulting in  $\mathcal{B} + \mathcal{H}$ . Then we impose the proposed identity-aware part-informed prompts  $\mathcal{P}$  on  $\mathcal{B}$ . Finally, the contribution of hierarchical fusion-based alignment  $\mathcal{F}$  is evaluated with  $\mathcal{B} + \mathcal{H} + \mathcal{F}$ , *i.e.*, the full version of our  $\pi$ -VL.

Table 3. Evaluation of each module on the DukeMTMC dataset.  $\mathcal{B}$ : the baseline model,  $\mathcal{H}$ : human parsing-based prompts,  $\mathcal{P}$ : identity-aware part-informed prompts,  $\mathcal{F}$ : hierarchical fusion-based alignment.

$\mathcal{B}$	$\mathcal{H}$	$\mathcal{P}$	$\mathcal{F}$	Rank-1	mAP
✓				89.4	80.8
✓	✓			90.2 (+0.8)	80.9 (+0.1)
✓		✓		91.0 (+1.6)	81.3 (+0.5)
✓		✓	✓	91.2 (+1.8)	81.6 (+0.8)

**Effectiveness of part-informed semantic labels.** As listed in Table 3, when only exploiting the human parsing labels as text prompts to perform image-text alignment, it surprisingly yields 0.8% gains of Rank-1 and 0.1% enhancement of mAP. This clearly suggests that fine-grained image-text alignment generally enriches the semantics of visual features. Unlike other part feature learning methods [44, 53], our fine-grained image-text alignment brings no additional inference costs to  $\mathcal{B}$ , which is highly efficient during model inference.

**Effectiveness of identity-aware part prompts.** A limitation of parsing label-based prompts is that human parsing only distinguishes the semantics of different body parts, while ReID needs to learn identity-related cues for person retrieval. Thus, we propose to combine identity and parsing prompts for image-text alignment. As proven by the 3rd row of Table 3, we get 0.8% gains of Rank-1 and 0.4% boost of mAP with the introduction of identity labels. Our method designs a *coarse-to-fine* fashion that first learns identity-specific prompts and then fits part semantics accordingly.

**Effectiveness of hierarchical fusion-based alignment.** With hierarchical fusion-based alignment, visual features from different stages can directly receive the supervision of natural language. Thus, it brings 0.2% Rank-1 and 0.3% mAP improvements over  $\mathcal{B} + \mathcal{P}$ , forming a more discriminative feature space for high-accuracy image retrieval.

Table 4. Generalization ability to different human parsing models.

Method	mIOU on [16]	Rank-1	mAP
CLIP-ReID [27] (baseline)	-	89.4	80.8
SOLIDER [4]	55.45	91.0	80.8
SCHP [26]	59.36	91.2	81.6
InVPT [55]	67.61	91.2	81.8

**Influence of different human parsing models.** A major concern for parsing-based ReID models is that the performance is sensitive to the quality of parsing maps. Here, we compare the ReID performance of  $\pi$ -VL with different hu-

man parsing models, including SOLIDER [4], InvPT [55], and SCHP [26], on the DukeMTMC dataset. As shown in Table 4, we observe consistent performance gains over the baseline model with different human parsing approaches. Besides, when equipped with different parsing models, the ReID performance of  $\pi$ -VL is highly stable. This is probably because our image-text alignment is conducted on the feature map level rather than the raw pixel level. The down-sampling operation can effectively erase several outliers in parsing maps. Moreover, since  $\pi$ -VL only involves human parsing in the training process, we can generate high-quality parsing maps in an offline manner to eliminate the label noises of visual-language learning.

#### 4.5. Transfer Ability of Part-informed Prompts

In this subsection, we investigate the transfer ability of the learned part-informed text prompts. Specifically, we first leverage the image and text encoders of CLIP for prompt tuning, and then adopt a light-weight network [41] pretrained on ImageNet [7] to conduct supervised ReID in the second training stage. This can be viewed as prompt-based knowledge distillation between the text encoder and the light-weight vision backbones. The experimental results on Market-1501 are listed in Table 5.

Table 5. Transfer ability of part-informed prompts.

Teacher	Student	Rank-1	mAP
CLIP-ReID [27]	-	95.7	89.8
$\pi$ -VL	-	96.1	90.2
-	MobileNetV2(0.25) [41]	85.0	66.9
CLIP-ReID [27]	MobileNetV2(0.25) [41]	86.2(+1.2)	67.8(+0.9)
$\pi$ -VL	MobileNetV2(0.25) [41]	87.1(+2.1)	68.5(+1.6)

We observe that visual-language learning significantly boosts the performance of the light-weight student network. This verifies that the learned text prompts are generalizable to different visual encoders and do improve the semantics of visual features (+1.2% Rank-1 and +0.9% mAP). Furthermore, compared with global identity prompts, our part-informed prompts present better generalization ability to downstream ReID tasks (+2.1% Rank-1 and +1.6% mAP). This further demonstrates the superiority of fine-grained prompt tuning and image-text alignment.

#### 4.6. Visualization Results

We further visualize the class activation map (CAM) [63] of 4 random queries from Market-1501 (Fig.5). It can be observed that the baseline model overlooks some significant visual cues for person ReID, *e.g.*, the face and shoes in 1st and 2nd columns, trousers in 3rd and 4th columns. The small number of captured cues may be insufficient for distinguishing different persons. Compare with the baseline, the proposed method form a full-scale characteristic of each identity by part-informed visual-language learning,

*e.g.*, faces, shirts, skirts, and shoulder bags. This indicates that fine-grained descriptions of body parts do provide a broader source of supervision than global identity-aware text prompts. Moreover, when there exists high background clutter, our approach is still superior to the baseline model in capturing identity-related cues. For instance, in the 1st column of Fig.5,  $\pi$ -VL accurately highlights the whole human body against irrelevant objects (*e.g.*, the white car and the bicycle). We also discover that all people’s shoes are spotlighted by  $\pi$ -VL. As an important personal belonging for ReID, this phenomenon further indicates that our method effectively enhances the fine-grained semantic information of visual features.

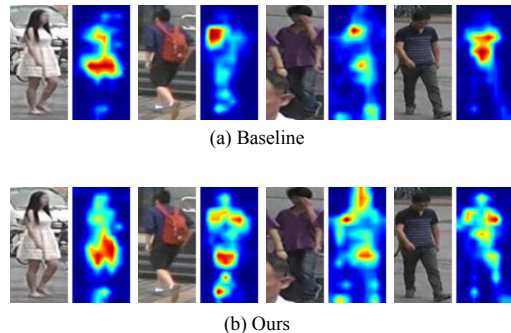


Figure 5. Visualization of class activation maps learned by  $\pi$ -VL and the baseline method [27]. Each instance is randomly sampled from the Market-1501 dataset. Bright colors illustrate the main focus of the model. Best viewed in color.

### 5. Conclusion

In this paper, we present one of the first attempts to extend visual-language learning-based ReID beyond the whole-body level to the fine-grained part level. Motivated by the within-part semantic inconsistency problem, we leverage human parsing to generate pixel-level semantic labels and design identity-aware part-informed text prompts based on the parsing maps. This enables us to perform fine-grained image-text alignment to construct a more semantic meaningful embedding space for person ReID. To cover visual features with different semantic levels, we also develop a simple-yet-effective feature pyramid network for visual feature fusion. The result of the above innovations,  $\pi$ -VL, is a plug-and-play and inference-free solution to general ReID tasks, which is highly compatible with modern backbone architectures. Experimental results and ablation studies on both CNN and ViT-based backbones demonstrate the superiority of the proposed  $\pi$ -VL approach over previous state-of-the-arts. And fine-grained visual-language learning is a promising research direction for general ReID tasks.

**Acknowledgments.** This work was supported by the National Key R&D Program of China (2022YFB4500600). The authors thank Hu Cheng, Chaolong Li, and Jinrui Shen for helpful discussions.

## References

- [1] Alberto Baldradi, Marco Bertini, Tiberio Uricchio, and Alberto Del Bimbo. Effective conditioned and composed image retrieval combining clip-based features. In *Proceedings of the IEEE/CVF Conference on Computer Vision and Pattern Recognition*, pages 21466–21474, 2022. 3
- [2] Tianlong Chen, Shaojin Ding, Jingyi Xie, Ye Yuan, Wuyang Chen, Yang Yang, Zhou Ren, and Zhangyang Wang. Abdnnet: Attentive but diverse person re-identification. In *Proceedings of the IEEE/CVF international conference on computer vision*, pages 8351–8361, 2019. 6, 7
- [3] Weihua Chen, Xiaotang Chen, Jianguo Zhang, and Kaiqi Huang. Beyond triplet loss: a deep quadruplet network for person re-identification. In *Proceedings of the IEEE Conference on Computer Vision and Pattern Recognition*, pages 403–412, 2017. 2
- [4] Weihua Chen, Xianzhe Xu, Jian Jia, Hao Luo, Yaohua Wang, Fan Wang, Rong Jin, and Xiuyu Sun. Beyond appearance: a semantic controllable self-supervised learning framework for human-centric visual tasks. In *Proceedings of the IEEE/CVF Conference on Computer Vision and Pattern Recognition*, pages 15050–15061, 2023. 1, 7, 8
- [5] Ying-Cong Chen, Xiatian Zhu, Wei-Shi Zheng, and Jian-Huang Lai. Person re-identification by camera correlation aware feature augmentation. *IEEE transactions on pattern analysis and machine intelligence*, 40(2):392–408, 2017. 2
- [6] Navneet Dalal and Bill Triggs. Histograms of oriented gradients for human detection. In *2005 IEEE computer society conference on computer vision and pattern recognition (CVPR'05)*, volume 1, pages 886–893. IEEE, 2005. 2
- [7] Jia Deng, Wei Dong, Richard Socher, Li-Jia Li, Kai Li, and Li Fei-Fei. Imagenet: A large-scale hierarchical image database. In *2009 IEEE conference on computer vision and pattern recognition*, pages 248–255. Ieee, 2009. 8
- [8] Alexey Dosovitskiy, Lucas Beyer, Alexander Kolesnikov, Dirk Weissenborn, Xiaohua Zhai, Thomas Unterthiner, Mostafa Dehghani, Matthias Minderer, Georg Heigold, Sylvain Gelly, et al. An image is worth 16x16 words: Transformers for image recognition at scale. *arXiv preprint arXiv:2010.11929*, 2020. 5
- [9] Shuguang Dou, Cairong Zhao, Xinyang Jiang, Shanshan Zhang, Wei-Shi Zheng, and Wangmeng Zuo. Human co-parsing guided alignment for occluded person re-identification. *IEEE Transactions on Image Processing*, 32:458–470, 2022. 2
- [10] Peng Gao, Shijie Geng, Renrui Zhang, Teli Ma, Rongyao Fang, Yongfeng Zhang, Hongsheng Li, and Yu Qiao. Clip-adapter: Better vision-language models with feature adapters. *arXiv preprint arXiv:2110.04544*, 2021. 3
- [11] Xinqian Gu, Hong Chang, Bingpeng Ma, Shutao Bai, Shiguang Shan, and Xilin Chen. Clothes-changing person re-identification with rgb modality only. In *Proceedings of the IEEE/CVF Conference on Computer Vision and Pattern Recognition*, pages 1060–1069, 2022. 6, 7
- [12] Xiuye Gu, Tsung-Yi Lin, Weicheng Kuo, and Yin Cui. Open-vocabulary object detection via vision and language knowledge distillation. *arXiv preprint arXiv:2104.13921*, 2021. 3
- [13] Yanming Guo, Yu Liu, Theodoros Georgiou, and Michael S Lew. A review of semantic segmentation using deep neural networks. *International journal of multimedia information retrieval*, 7:87–93, 2018. 3
- [14] Kaiming He, Xiangyu Zhang, Shaoqing Ren, and Jian Sun. Deep residual learning for image recognition. In *Proceedings of the IEEE conference on computer vision and pattern recognition*, pages 770–778, 2016. 3, 5, 6
- [15] Shuting He, Hao Luo, Pichao Wang, Fan Wang, Hao Li, and Wei Jiang. Transreid: Transformer-based object re-identification. In *Proceedings of the IEEE/CVF international conference on computer vision*, pages 15013–15022, 2021. 1, 6, 7
- [16] Derek Hoiem, Santosh K Divvala, and James H Hays. Pascal voc 2008 challenge. *World Literature Today*, 24(1), 2009. 7
- [17] Ruibing Hou, Bingpeng Ma, Hong Chang, Xinqian Gu, Shiguang Shan, and Xilin Chen. Interaction-and-aggregation network for person re-identification. In *Proceedings of the IEEE Conference on Computer Vision and Pattern Recognition*, pages 9317–9326, 2019. 2
- [18] Chao Jia, Yinfei Yang, Ye Xia, Yi-Ting Chen, Zarana Parekh, Hieu Pham, Quoc Le, Yun-Hsuan Sung, Zhen Li, and Tom Duerig. Scaling up visual and vision-language representation learning with noisy text supervision. In *International conference on machine learning*, pages 4904–4916. PMLR, 2021. 3
- [19] Xin Jin, Cuiling Lan, Wenjun Zeng, Guoqiang Wei, and Zhibo Chen. Semantics-aligned representation learning for person re-identification. In *Proceedings of the AAAI Conference on Artificial Intelligence*, volume 34, pages 11173–11180, 2020. 6, 7
- [20] Mahdi M Kalayeh, Emrah Basaran, Muhittin Gökmen, Mustafa E Kamasak, and Mubarak Shah. Human semantic parsing for person re-identification. In *Proceedings of the IEEE Conference on Computer Vision and Pattern Recognition*, pages 1062–1071, 2018. 2
- [21] Srikrishna Karanam, Yang Li, and Richard J Radke. Person re-identification with discriminatively trained viewpoint invariant dictionaries. In *Proceedings of the IEEE international conference on computer vision*, pages 4516–4524, 2015. 2
- [22] Wonjae Kim, Bokyoung Son, and Ildoo Kim. Vilt: Vision-and-language transformer without convolution or region supervision. In *International Conference on Machine Learning*, pages 5583–5594. PMLR, 2021. 3
- [23] Hanjun Li, Gaojie Wu, and Wei-Shi Zheng. Combined depth space based architecture search for person re-identification. In *Proceedings of the IEEE/CVF Conference on Computer Vision and Pattern Recognition*, pages 6729–6738, 2021. 6, 7
- [24] Junnan Li, Dongxu Li, Caiming Xiong, and Steven Hoi. Blip: Bootstrapping language-image pre-training for unified vision-language understanding and generation. In *International Conference on Machine Learning*, pages 12888–12900. PMLR, 2022. 1, 3

- [25] Junnan Li, Ramprasaath Selvaraju, Akhilesh Gotmare, Shafiq Joty, Caiming Xiong, and Steven Chu Hong Hoi. Align before fuse: Vision and language representation learning with momentum distillation. *Advances in neural information processing systems*, 34:9694–9705, 2021. [3](#)
- [26] Peike Li, Yunqiu Xu, Yunchao Wei, and Yi Yang. Self-correction for human parsing. *IEEE Transactions on Pattern Analysis and Machine Intelligence*, 44(6):3260–3271, 2020. [2](#), [4](#), [7](#), [8](#)
- [27] Siyuan Li, Li Sun, and Qingli Li. Clip-reid: Exploiting vision-language model for image re-identification without concrete text labels. In *Proceedings of the AAAI Conference on Artificial Intelligence*, volume 37, pages 1405–1413, 2023. [1](#), [3](#), [4](#), [6](#), [7](#), [8](#)
- [28] Wei Li, Xi Tian Zhu, and Shaogang Gong. Harmonious attention network for person re-identification. In *Proceedings of the IEEE conference on computer vision and pattern recognition*, pages 2285–2294, 2018. [2](#)
- [29] Yulin Li, Jianfeng He, Tianzhu Zhang, Xiang Liu, Yongdong Zhang, and Feng Wu. Diverse part discovery: Occluded person re-identification with part-aware transformer. In *Proceedings of the IEEE/CVF Conference on Computer Vision and Pattern Recognition*, pages 2898–2907, 2021. [2](#), [6](#), [7](#)
- [30] Yanghao Li, Hanzi Mao, Ross Girshick, and Kaiming He. Exploring plain vision transformer backbones for object detection. In *European Conference on Computer Vision*, pages 280–296. Springer, 2022. [5](#)
- [31] Shengcai Liao, Yang Hu, Xiangyu Zhu, and Stan Z Li. Person re-identification by local maximal occurrence representation and metric learning. In *Proceedings of the IEEE conference on computer vision and pattern recognition*, pages 2197–2206, 2015. [2](#)
- [32] Tsung-Yi Lin, Piotr Dollár, Ross Girshick, Kaiming He, Bharath Hariharan, and Serge Belongie. Feature pyramid networks for object detection. In *Proceedings of the IEEE conference on computer vision and pattern recognition*, pages 2117–2125, 2017. [5](#)
- [33] Chuanchen Luo, Yuntao Chen, Naiyan Wang, and Zhaoxiang Zhang. Spectral feature transformation for person re-identification. In *Proceedings of the IEEE International Conference on Computer Vision*, pages 4976–4985, 2019. [2](#)
- [34] Hao Luo, Youzhi Gu, Xingyu Liao, Shenqi Lai, and Wei Jiang. Bag of tricks and a strong baseline for deep person re-identification. In *Proceedings of the IEEE/CVF Conference on Computer Vision and Pattern Recognition (CVPR) Workshops*, June 2019. [1](#), [2](#), [3](#), [6](#)
- [35] Jiayu Miao, Yu Wu, Ping Liu, Yuhang Ding, and Yi Yang. Pose-guided feature alignment for occluded person re-identification. In *Proceedings of the IEEE International Conference on Computer Vision*, pages 542–551, 2019. [2](#), [5](#), [6](#)
- [36] Aaron van den Oord, Yazhe Li, and Oriol Vinyals. Representation learning with contrastive predictive coding. *arXiv preprint arXiv:1807.03748*, 2018. [3](#)
- [37] Ruijie Quan, Xuanyi Dong, Yu Wu, Linchao Zhu, and Yi Yang. Auto-reid: Searching for a part-aware convnet for person re-identification. In *Proceedings of the IEEE/CVF International Conference on Computer Vision*, pages 3750–3759, 2019. [1](#), [6](#), [7](#)
- [38] Alec Radford, Jong Wook Kim, Chris Hallacy, Aditya Ramesh, Gabriel Goh, Sandhini Agarwal, Girish Sastry, Amanda Askell, Pamela Mishkin, Jack Clark, et al. Learning transferable visual models from natural language supervision. In *International conference on machine learning*, pages 8748–8763. PMLR, 2021. [1](#), [2](#), [3](#), [6](#)
- [39] Yongming Rao, Wenliang Zhao, Guangyi Chen, Yansong Tang, Zheng Zhu, Guan Huang, Jie Zhou, and Jiwen Lu. Denseclip: Language-guided dense prediction with context-aware prompting. In *Proceedings of the IEEE/CVF Conference on Computer Vision and Pattern Recognition*, pages 18082–18091, 2022. [3](#)
- [40] Ergys Ristani, Francesco Solera, Roger Zou, Rita Cucchiara, and Carlo Tomasi. Performance measures and a data set for multi-target, multi-camera tracking. In *European conference on computer vision*, pages 17–35. Springer, 2016. [4](#), [5](#), [6](#)
- [41] Mark Sandler, Andrew Howard, Menglong Zhu, Andrey Zhmoginov, and Liang-Chieh Chen. Mobilenetv2: Inverted residuals and linear bottlenecks. In *Proceedings of the IEEE conference on computer vision and pattern recognition*, pages 4510–4520, 2018. [5](#), [8](#)
- [42] Yantao Shen, Hongsheng Li, Shuai Yi, Dapeng Chen, and Xiaogang Wang. Person re-identification with deep similarity-guided graph neural network. In *Proceedings of the European conference on computer vision (ECCV)*, pages 486–504, 2018. [2](#)
- [43] Chunfeng Song, Yan Huang, Wanli Ouyang, and Liang Wang. Mask-guided contrastive attention model for person re-identification. In *Proceedings of the IEEE conference on computer vision and pattern recognition*, pages 1179–1188, 2018. [2](#)
- [44] Yifan Sun, Liang Zheng, Yi Yang, Qi Tian, and Shengjin Wang. Beyond part models: Person retrieval with refined part pooling (and a strong convolutional baseline). In *Proceedings of the European Conference on Computer Vision (ECCV)*, September 2018. [1](#), [2](#), [6](#), [7](#)
- [45] Hongchen Tan, Xiuping Liu, Yuhao Bian, Huasheng Wang, and Baocai Yin. Incomplete descriptor mining with elastic loss for person re-identification. *IEEE Transactions on Circuits and Systems for Video Technology*, 32(1):160–171, 2021. [6](#), [7](#)
- [46] Laurens Van der Maaten and Geoffrey Hinton. Visualizing data using t-sne. *Journal of machine learning research*, 9(11), 2008. [4](#)
- [47] Ashish Vaswani, Noam Shazeer, Niki Parmar, Jakob Uszkoreit, Llion Jones, Aidan N Gomez, Łukasz Kaiser, and Illia Polosukhin. Attention is all you need. *Advances in neural information processing systems*, 30, 2017. [6](#)
- [48] Guan’an Wang, Shuo Yang, Huanyu Liu, Zhicheng Wang, Yang Yang, Shuliang Wang, Gang Yu, Erjin Zhou, and Jian Sun. High-order information matters: Learning relation and topology for occluded person re-identification. In *Proceedings of the IEEE/CVF Conference on Computer Vision and Pattern Recognition*, pages 6449–6458, 2020. [2](#), [6](#), [7](#)
- [49] Guanshuo Wang, Yufeng Yuan, Xiong Chen, Jiwei Li, and Xi Zhou. Learning discriminative features with multiple gran-

- ularities for person re-identification. In *Proceedings of the 26th ACM international conference on Multimedia*, pages 274–282, 2018. [1](#), [4](#), [6](#), [7](#)
- [50] Pingyu Wang, Zhicheng Zhao, Fei Su, and Honying Meng. Ltreid: Factorizable feature generation with independent components for long-tailed person re-identification. *IEEE Transactions on Multimedia*, 2022. [6](#), [7](#)
- [51] Xinlong Wang, Rufeng Zhang, Chunhua Shen, Tao Kong, and Lei Li. Dense contrastive learning for self-supervised visual pre-training. In *Proceedings of the IEEE/CVF Conference on Computer Vision and Pattern Recognition*, pages 3024–3033, 2021. [5](#)
- [52] Zhongdao Wang, Liang Zheng, Yixuan Liu, Yali Li, and Shengjin Wang. Towards real-time multi-object tracking. In *European Conference on Computer Vision*, pages 107–122. Springer, 2020. [2](#), [4](#)
- [53] Longhui Wei, Shiliang Zhang, Wen Gao, and Qi Tian. Person transfer gan to bridge domain gap for person re-identification. In *Proceedings of the IEEE conference on computer vision and pattern recognition*, pages 79–88, 2018. [2](#), [5](#), [7](#)
- [54] Yichao Yan, Jie Qin, Bingbing Ni, Jiabin Chen, Li Liu, Fan Zhu, Wei-Shi Zheng, Xiaokang Yang, and Ling Shao. Learning multi-attention context graph for group-based re-identification. *IEEE Transactions on Pattern Analysis and Machine Intelligence*, 2020. [2](#)
- [55] Hanrong Ye and Dan Xu. Invt: Inverted pyramid multi-task transformer for dense scene understanding. *arXiv preprint arXiv:2203.07997*, 2022. [2](#), [7](#), [8](#)
- [56] Mang Ye, Jianbing Shen, Gaojie Lin, Tao Xiang, Ling Shao, and Steven CH Hoi. Deep learning for person re-identification: A survey and outlook. *IEEE transactions on pattern analysis and machine intelligence*, 44(6):2872–2893, 2021. [1](#), [2](#)
- [57] Zelong Zeng, Zhixiang Wang, Zheng Wang, Yinqiang Zheng, Yung-Yu Chuang, and Shin’ichi Satoh. Illumination-adaptive person re-identification. *IEEE Transactions on Multimedia*, 2020. [2](#)
- [58] Enwei Zhang, Xinyang Jiang, Hao Cheng, Ancong Wu, Fufu Yu, Ke Li, Xiaowei Guo, Feng Zheng, Weishi Zheng, and Xing Sun. One for more: Selecting generalizable samples for generalizable reid model. In *Proceedings of the AAAI Conference on Artificial Intelligence*, volume 35, pages 3324–3332, 2021. [6](#), [7](#)
- [59] Quan Zhang, Jianhuang Lai, Zhanxiang Feng, and Xiaohua Xie. Seeing like a human: Asynchronous learning with dynamic progressive refinement for person re-identification. *IEEE Transactions on Image Processing*, 31:352–365, 2021. [6](#), [7](#)
- [60] Liang Zheng, Liyue Shen, Lu Tian, Shengjin Wang, Jingdong Wang, and Qi Tian. Scalable person re-identification: A benchmark. In *Proceedings of the IEEE international conference on computer vision*, pages 1116–1124, 2015. [1](#), [5](#), [6](#)
- [61] Zhedong Zheng, Liang Zheng, and Yi Yang. Unlabeled samples generated by gan improve the person re-identification baseline in vitro. In *Proceedings of the IEEE international conference on computer vision*, pages 3754–3762, 2017. [1](#)
- [62] Zhun Zhong, Liang Zheng, Guoliang Kang, Shaozi Li, and Yi Yang. Random erasing data augmentation. In *Proceedings of the AAAI conference on artificial intelligence*, volume 34, pages 13001–13008, 2020. [6](#)
- [63] Bolei Zhou, Aditya Khosla, Agata Lapedriza, Aude Oliva, and Antonio Torralba. Learning deep features for discriminative localization. In *Proceedings of the IEEE conference on computer vision and pattern recognition*, pages 2921–2929, 2016. [8](#)
- [64] Kaiyang Zhou, Jingkang Yang, Chen Change Loy, and Ziwei Liu. Conditional prompt learning for vision-language models. In *Proceedings of the IEEE/CVF Conference on Computer Vision and Pattern Recognition*, pages 16816–16825, 2022. [3](#)
- [65] Kaiyang Zhou, Jingkang Yang, Chen Change Loy, and Ziwei Liu. Learning to prompt for vision-language models. *International Journal of Computer Vision*, 130(9):2337–2348, 2022. [1](#), [3](#), [4](#)
- [66] Kaiyang Zhou, Yongxin Yang, Andrea Cavallaro, and Tao Xiang. Omni-scale feature learning for person re-identification. In *Proceedings of the IEEE/CVF international conference on computer vision*, pages 3702–3712, 2019. [1](#), [6](#), [7](#)
- [67] Haowei Zhu, Wenjing Ke, Dong Li, Ji Liu, Lu Tian, and Yi Shan. Dual cross-attention learning for fine-grained visual categorization and object re-identification. In *Proceedings of the IEEE/CVF Conference on Computer Vision and Pattern Recognition*, pages 4692–4702, 2022. [6](#), [7](#)
- [68] Kuan Zhu, Haiyun Guo, Zhiwei Liu, Ming Tang, and Jinqiao Wang. Identity-guided human semantic parsing for person re-identification. In *Computer Vision—ECCV 2020: 16th European Conference, Glasgow, UK, August 23–28, 2020, Proceedings, Part III 16*, pages 346–363. Springer, 2020. [6](#), [7](#)
- [69] Kuan Zhu, Haiyun Guo, Shiliang Zhang, Yaowei Wang, Gaopan Huang, Honglin Qiao, Jing Liu, Jinqiao Wang, and Ming Tang. Aaformer: Auto-aligned transformer for person re-identification. *arXiv preprint arXiv:2104.00921*, 2021. [6](#), [7](#)
- [70] Jialong Zuo, Changqian Yu, Nong Sang, and Changxin Gao. Plip: Language-image pre-training for person representation learning. *arXiv preprint arXiv:2305.08386*, 2023. [2](#)